1st IMEKO TC-4 International Workshop on
Metrology for Geotechnics
Benevento, Italy, March 17-18, 2016

Seismic behaviour of large earth dams: from site investigations to numerical modelling

Luca Masini, Sebastiano Rampello, Luigi Callisto

"Sapienza", Università di Roma, luca.masini@uniroma1.it

***Abstract* – This paper presents selected results from the study on the seismic behaviour of a large earth dam. The study relies on the availability of field and laboratory tests, as well as on monitoring data collected during the construction and impounding phases. Specifically, a two-dimensional numerical model was calibrated by comparing the settlements of the dam measured during the construction with the computed values. Iterative pseudo-static numerical analyses were carried out to investigate the plastic mechanisms forming under critical conditions. The seismic performance of the dam was then evaluated through a series of dynamic analyses in terms of effective stress. The results evidenced that a significant reduction of the seismic energy is obtained if the deformability of the bedrock is accounted for in the analyses, resulting in lower permanent displacements of the dam body, and, conversely, the vertical component of the seismic action induces a sensible increase of the seismic displacements.**

I. LAYOUT OF THE PROBLEM

The seismic behaviour of large earth dams is strongly affected by the inertial forces that develop during the ground motion, varying with time and space. The distribution and evolution of these forces depend on the characteristics of the embankment and the foundation soil, the effective stress state induced by construction and impounding phases as well as on the geometry of the dam.

The traditional approaches of analysis, based on a number of simplifying assumptions, are able to take into account only some of the above mentioned factors. Dynamic non-linear numerical analyses, carried out in two or three-dimensional conditions are capable of a more accurate description of the seismic response of the dam, provided that the numerical model is calibrated correctly. Moreover, they permit to follow the evolution with time of the stress state and of the deformation pattern within the earth dam.

This study focuses on the seismic behaviour of large earth dams and in this paper some preliminary results are discussed. Specifically, numerical analyses were carried out with the finite difference code FLAC v.5.0 [1] using a numerical model that was conceived adopting some simplifying assumptions about the geometry of an existing homogeneous earth dam. This specific dam dikes the course of the Marana Capacciotti stream in Southern Italy and represents a well documented case-history in the literature [2,3,4,5,6], with a comprehensive geotechnical characterisation of the embankment and the foundation soil and monitoring data from the construction and the impounding phases [2].

Figure 1 shows the layout of the homogeneous embankment, that was converted into a plane-strain numerical model. The dam has a height $H = 50$ m, a width of 400 m and the slope of the flanks is $\alpha = 14°$. The drainage system consists of a sub-vertical central drain and of a horizontal drain located at the toe of the downstream slope. Seepage through the 15 m-high alluvial deposit underlying the dam is prevented by an impervious diaphragm extending into the lower firm soil.

The strength and stiffness properties of the soils were obtained from the geotechnical investigations carried out throughout the earth dam and the foundation soils, as comprehensively reported by Calabresi *et al.* [2]. Specifically, three boreholes and four cone penetration tests were carried out from the crest and the downstream bank of the dam, and laboratory tests were performed on 21 undisturbed tube samples.

Table 1 lists the stiffness and shear strength parameters adopted in the analyses. The effective friction angle, φ', and cohesion, c', were obtained from standard consolidated undrained triaxial compression tests and drained direct shear tests.

The small strain shear modulus G_0 was expressed as a function of the mean effective stress p':

$$G_0 = A + B \cdot \left(\frac{p'}{p_r} \right)^n \qquad (1)$$

where $p_r = 1$ kPa is a reference pressure. Values for the coefficients A, B, and n were selected to fit the measurements of G_0 obtained from resonant column tests carried out on the undisturbed samples retrieved from the dam body and the foundation soil [2]. The stiff clay deposit found underneath the alluvial soil was regarded as a bedrock characterised by a shear wave velocity $V_s = 1000$ m/s, with constant small strain shear modulus $G_0 = 2060$ MPa and bulk modulus $K = 5026$ MPa.

ISBN: 978-92-990075-0-1

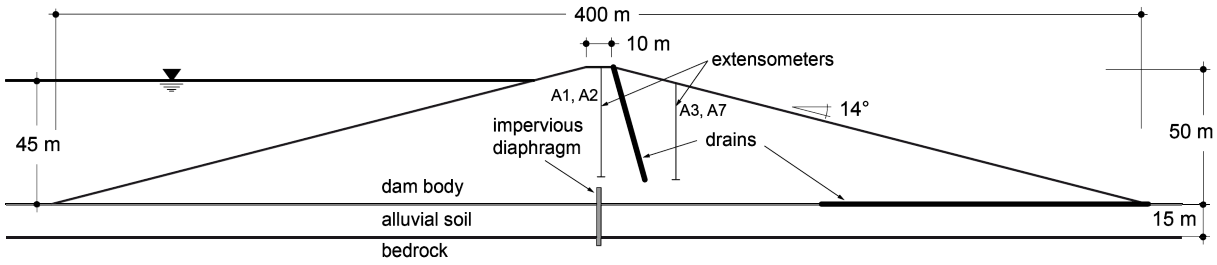

Fig. 1. Layout of the homogeneous earth dam and location of the extensometers.

Table 1. Mechanical properties of soil.

soil	γ (kN/m^3)	*c*' (kPa)	φ' (°)	ψ (°)	k_0 (-)	k (m/s)	*A* (MPa)	*B* (MPa)	*n*	ν
dam body	20.8	20	28	0	-	10^{-7}	19.476	1573	0.75	0.30
foundation soil	20.6	7	32	0	1.5	10^{-6}	19.476	2155	0.73	0.32
bedrock	20.6	-	-	-	1.5	10^{-9}	2060	0	-	0.32

Table 2. Properties of the input seismic records.

record	a_{max} (***g***)	I_a (m/s)	T_s (s)	T_m (s)
Tolmezzo NS (*F*=1)	0.357	0.790	4.31	0.393
Tolmezzo V (*F*=1)	0.267	0.334	5.16	0.211
Tolmezzo NS (*F*=1.8)	0.642	2.561	4.31	0.393
Tolmezzo V (F=1.8)	0.480	1.084	5.16	0.211

II. 1D SEISMIC RESPONSE ANALYSIS

The dynamic response of the numerical model was preliminary calibrated by comparing the results of free-field 1D FLAC simulations to those obtained using the code MARTA v.1.1.06 [7], in which the soil is modelled as a linear equivalent viscous-elastic material. Specifically, a 67 m-height column of soil was assumed as representative of the soil sequence at the dam centreline: from the ground surface, the first 50 m-thick layer represents the dam body that overlies the foundation soil. The latter consists of an alluvial deposit 15 m thick resting over the bedrock, which was modelled as an elastic layer with a thickness of 2 m in order to simulate, using the FLAC "quiet" (viscous) boundary conditions, an elastic halfspace.

In the dynamic analyses, the dam body and the foundation soil were modelled as non-linear elastic-perfectly plastic materials with Mohr-Coulomb's plasticity criterion and zero dilatancy angle, ψ.

The cyclic behaviour of the soil was described through the hysteretic damping model Sigmoidal4, implemented in FLAC. This is essentially an extension to two dimensions of the non-linear soil models that describe the unloading–reloading stress–strain cycles using Masing's rules. The model requires the value of the small-strain shear stiffness G_0 and a backbone curve. As previously discussed, the small-strain shear stiffness was expressed as a function of the mean effective stress, while the backbone curve was calibrated to reproduce the modulus decay curves obtained from the resonant column (RC) tests performed on samples retrieved from the dam body and the foundation soil [2]. Figure 2 shows a comparison between the prediction of the hysteretic model and the modulus decay curves obtained from RC tests. For high values of the shear strain γ, the experimental results for the dam body were integrated with the G/G_0-γ equation proposed by Ishibashi and Zang [8] assuming a mean effective stress $p' = 50$ kPa and a plasticity index PI = 0, while those for the foundation soil were integrated with the curve published by Seed and Idriss [9].

A small amount of additional damping was introduced in the FLAC analyses to attenuate the soil response at very small strains and to reduce spurious high-frequency noise. This was obtained by specifying a frequency independent "local" damping ratio equal to 0.5%. A real seismic record was used as input motion, selected from a set of events compatible with the seismicity of the site [3]. Specifically, the North-South and the vertical components of Tolmezzo station record (Friuli 1976 earthquake) were used. In the 2D-simulations, the recorded accelerations were multiplied by a scaling factor $F = 1.8$ to match the elastic response spectrum of the newly-released Italian building code for dams [10], calculated for a return period $T_R = 2475$ years. Some properties of the records are reported in Table 2, where a_{max} is the peak ground acceleration, I_A is the Arias intensity, T_s is the significant duration and T_m is the mean quadratic period as defined by Rathje *et al*. [11].

The free-field seismic response analyses were carried out assuming an elastic bedrock, by applying to the base of the column a time history of shear stress τ_{xy} defined as:

$$\tau_{xy}(t) = \rho V_s \cdot \int a(t) \qquad (2)$$

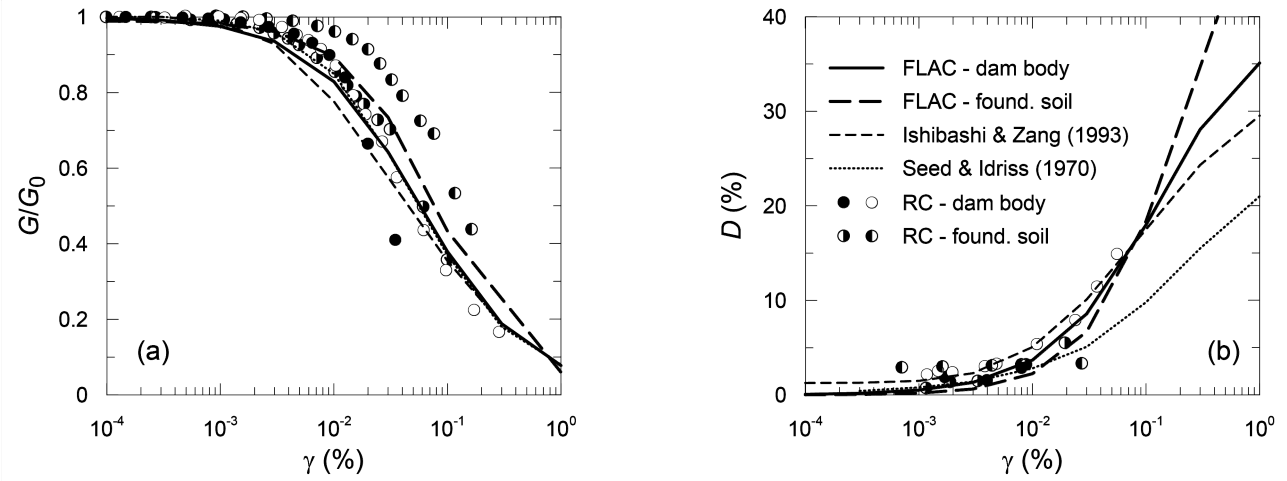

Fig. 2. Comparison between RC tests results and model simulations.

where ρ = 2.06 Mg/m^3 and V_S = 1000 m/s are the bedrock density and shear wave velocity, while $\int a(t)$ is the velocity obtained by integrating the horizontal component of the acceleration time history. FLAC "quiet" (viscous) boundary conditions were applied to the bottom of the grid while free-field boundary conditions were activated to the lateral sides, and the soil initial elastic stiffness was set equal to the small-strain stiffness.

Figure 3a,b,c show the results of FLAC 1D free-field analyses compared with those obtained using the code MARTA. The adopted shear wave velocity profile is also shown in Figure 3a. Similar values of the maximum horizontal acceleration $a_{x,max}$ were computed with both methods in the bedrock and the foundation soil (Figure 3b), while lower values were obtained in the dam body with the finite difference analysis, as the hysteretic model predicts a somewhat larger damping for γ > 0.1 %. Figure 3c shows the elastic response spectra computed at the base (h = 0 m), at about the middle (h = 20 m) and at the top (h = 50 m) of the dam body. Although the FLAC analysis emphasises high frequencies, the two methods are in a fair agreement to each other.

Additional FLAC analyses were carried out by taking into account the vertical component of the input motion by applying to the base of the column a time history of vertical stress

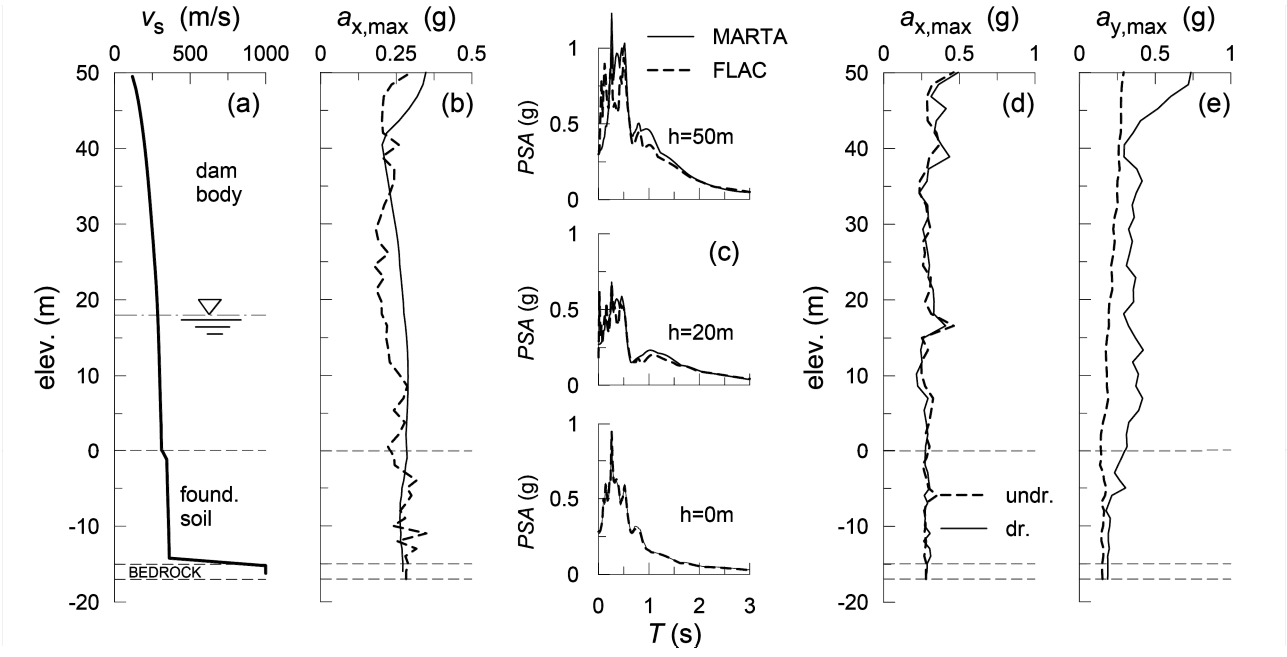

Fig. 3. Results of free-field analyses.

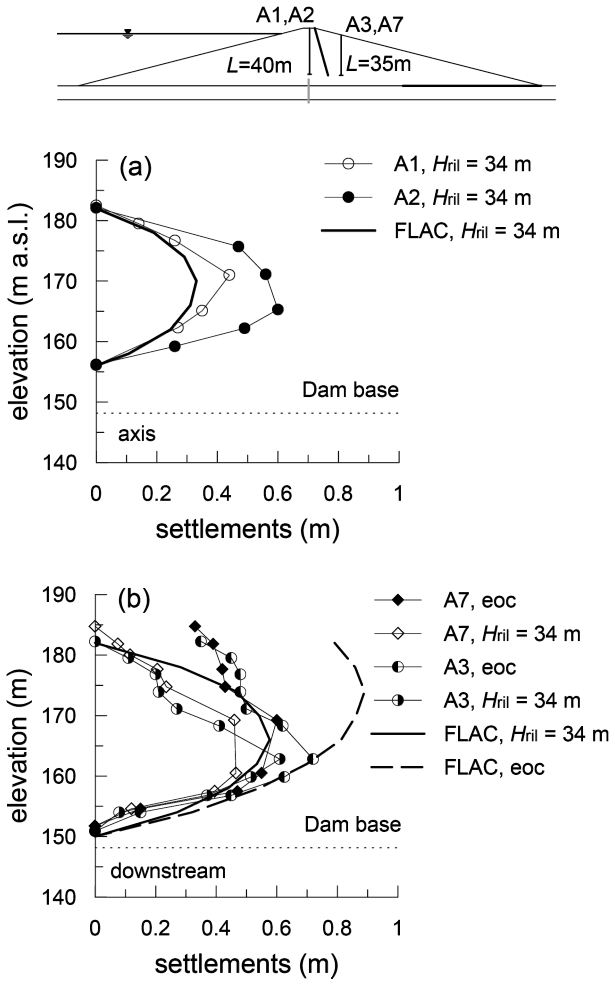

Fig. 4. Observed and computed settlement profile.

$$\sigma_{yy}(t) = \rho V_p \cdot \int a(t) \tag{3}$$

where V_p is the compression wave velocity at the bedrock, assumed equal to 2000 m/s. Both drained and undrained conditions were assumed in calculations. A water bulk modulus $K_w = 1$ GPa was assumed in the undrained analyses. Figures 3d-3e show the profiles of the maximum horizontal ($a_{x,max}$) and vertical ($a_{y,max}$) accelerations: while $a_{x,max}$ shows minor changes between drained and undrained conditions, a substantial increase of $a_{y,max}$ was computed assuming drained conditions because of the larger difference in dynamic impedances between the bedrock and the alluvial deposit. In the undrained analysis, in fact, the volumetric stiffness of the water- saturated embankment soil is similar to that of the bedrock, resulting in a lower amplification of $a_{y,max}$. However, for the case at hand, the assumption of fully drained conditions seems unlikely to occur as both the foundation layer and the dam body are made by fine grained soils.

III. 2D ANALYSES

Two-dimensional dynamic analyses were carried out in the time domain to study the seismic behaviour of the homogenous earth dam. Values used for the strength and stiffness parameters of soils are the same of the free-field analyses. To obtain a correct initial state of effective stress prior to the dynamic calculation phase, it is important to simulate the static construction of the dam, the impoundment phases and the unconfined seepage through the dam. This is needed to evaluate the G_0 distribution within the embankment and the foundation soil. To this aim, the staged construction of the dam, considered as a drained process, was modelled by progressively activating 13 embankment layers about 4m thick; the impounding of the reservoir and the associated steady-state seepage flow through the dam were simulated by raising the water level in three stages of 15 m, reaching the maximum storage level of 45 m. The shear stiffness values adopted for the static calculations were obtained reducing the small strain shear stiffness G_0 by a factor which was calibrated to reproduce the settlement profiles observed during construction and impounding phases. Specifically, as operative shear modulus, 5% of G_0 were used for the dam body and the foundation soil, while 0.5% of G_0 were used for the bedrock. Such a low operative shear modulus was needed to reproduce the absolute settlements observed at the base of dam, since the firm deposit was modelled as 2 a meters thick layer while a geological study of the site provides an estimate of the bedrock depth of about 300m. At the end of each calculation phase, the soil stiffness was updated to correspond to the new effective stress state. Model calibration was checked using the settlements measured during the dam construction via four extensometers installed at the centreline and in the downstream slope of the dam, as shown in Figure 1. The observed settlement profiles are shown in Figure 4 together with the computed ones; Figure 4a shows the settlement profiles along two vertical axes (A1 and A2) through the crest of the dam at a stage when the dam was not yet completed ($H = 34$m), while Figure 4b shows profiles along two vertical axes located on the downstream slope of the dam (A3 and A7) measured when $H = 34$m and at the end of construction ('eoc' in the figure). On the average, the results of the numerical analysis agree with the monitoring data. The observed increase in settlements at the top of extensometers A3, A7 is somewhat due to the construction of the overlying portion of the dam.

Starting from the end of construction and impounding phases, a pseudo-static analysis was carried out applying uniform horizontal body forces expressed as a fraction k_h of gravity g. The seismic coefficient k_h was increased progressively until convergence, evidenced by a steady reduction of the unbalanced forces, became no longer possible. Under this circumstance, the numerical model

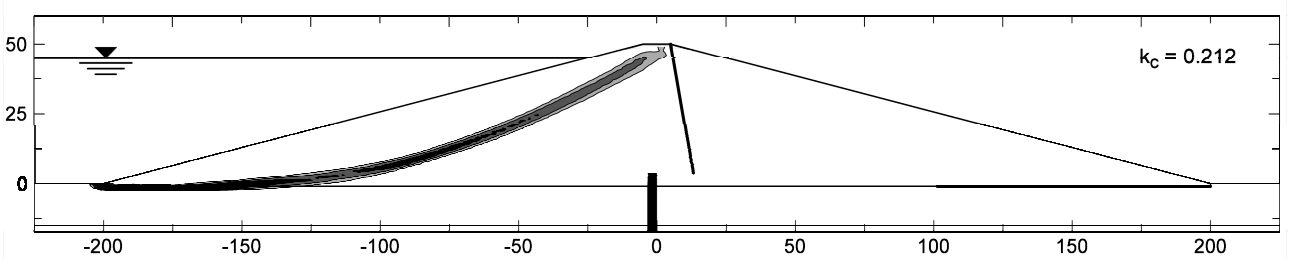

Fig. 5. Pseudo static analysis, contours of the shear strain rate computed for $k_h = k_c$.

exhibited a well-defined mechanism, associated with a plastic flow of the soil. The seismic coefficient k_h that activates the mechanism is termed 'critical' and is indicated as k_c. It was found [12] that the solution does not depend on the stiffness of the materials and therefore can be assumed as a result of the strength properties only. Therefore, the critical seismic coefficient k_c represents a measure of the global seismic resistance of the system. Since the pseudo-static analyses were carried out up to critical conditions, the values of the computed displacements are only conventional, as they refer to a system that is accelerating due to the static activation of a plastic mechanism.

Calculations were conducted for both directions of the horizontal component of the inertial force $k_h \cdot g$. As expected, the minimum value of the critical seismic coefficient ($k_c = 0.212$) was obtained when the pseudo-static force is oriented towards the upstream slope. Figure 5 shows the contours of the shear strain rate for $k_h = k_c$, indicating the activation of a plastic mechanism extending from the top to the toe of the embankment, on the upstream side, mainly consisting in the rotation of the unstable soil mass. This result is consistent with that obtained by Calabresi *et al.* [2] using the limit equilibrium method although they obtained a slightly smaller value ($k_c = 0.153$) as they assumed more conservative strength values ($c = 0'$, $\varphi' = 27°$).

Pseudo-static numerical analyses provide a first evaluation of the behaviour of the dam in presence of intense seismic loadings which are capable of mobilizing temporarily the shear strength of soil.

Starting from the end-of-construction stage, time-domain dynamic analyses were then carried out by applying time-histories of the input motion to the bottom boundary of the same finite difference grid used for the pseudo-static analyses. FLAC "quiet" (viscous) boundary conditions were activated to the lateral sides of the grid, and the initial soil stiffness was set equal to the small strain stiffness. Table 3 lists the different conditions assumed for each dynamic analysis. Calculations were conducted for both the assumptions of rigid and elastic bedrock. In the first case, time-histories of accelerations were applied to the bottom boundary, while, in the second, time-histories of stresses calculated from Eq. (2) and (3) were used. In analyses A, B, C, and D undrained conditions were assumed while in case E calculations were repeated for drained conditions.

Figure 6a shows the profiles of non-dimensional maximum acceleration along the dam centre line, where $a_{x,base}$ and $a_{y,base}$ are the maximum horizontal and vertical acceleration computed at the base of the dam, and $H = 50$ m is the dam height. Nearly constant values of $a_x / a_{x,base}$ were computed in the lower third of the embankment for all the analyses, while a small de-amplification occurred in the middle third, the minimum value ($a_x / a_{x,base} = 0.6$) being obtained for case A and E. Conversely, in the topmost third $a_x / a_{x,base}$ increases to about twice the value calculated at the base for all but case E, as seismic waves converge to the top of the dam. Although sensibly different values of $a_{x,max}$ were obtained for the four undrained analyses (case A to D, not shown here for brevity), the highest values being computed for case C, the profiles of the amplification factor do not seem to show a clear trend.

Values of $a_y / a_{y,base}$ larger than 1 were computed for the undrained analyses (case A to D) while a 20% de-amplification of the vertical acceleration was obtained for the drained analysis (case E). In fact, assuming undrained conditions, the high bulk modulus of water results in a response of the system which is globally more rigid for compressive loadings, leading to a larger amplification of both the acceleration components.

Figure 7a shows the horizontal displacement time histories computed in two points, one in the upstream slope (point K), the other in the downstream slope (point Q), for case C and D. Negative values indicate displacements towards the upstream slope. For case C, the horizontal displacements at the end of the ground shaking are -0.58 m and 0.25 m upstream and downstream, respectively. If the stiffness of the firm soil is accounted for (case D) a large reduction of the horizontal displacement is obtained upstream (0.10 m), while the downstream displacements are largely

Table 3. Case of analysis.

analysis	drainage	vert. comp.	bedrock
A	no	no	rigid
B	no	no	elastic
C	no	yes	rigid
D	no	yes	elastic
E	yes	no	rigid

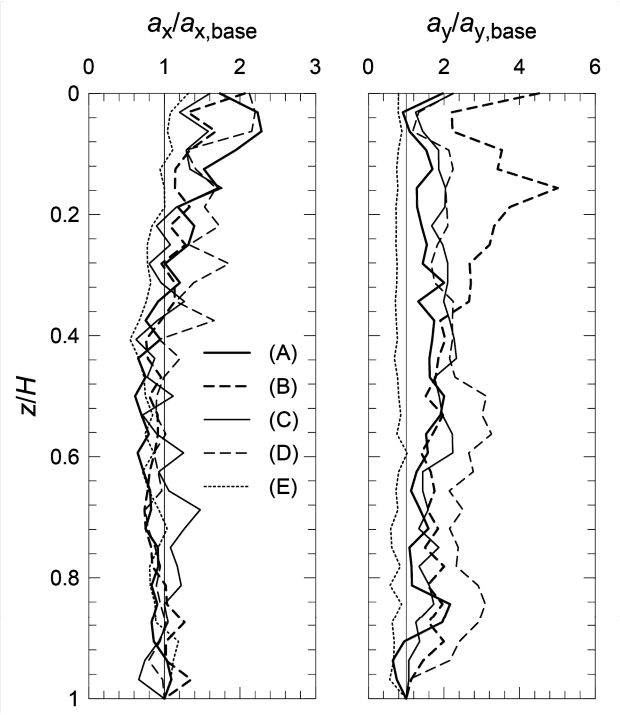

Fig. 6. Results of the 2D dynamic analyses.

unaffected. Permanent displacements result from the transient activation of plastic mechanisms during the earthquake; for case C they mainly involve the upstream slope, in agreement with the results of the pseudo-static analysis. Therefore, the final permanent displacements are influenced by the duration of the strong motion phase of the input motion, represented by the two dashed vertical lines of Figure 7. In Figure 7b the horizontal displacements computed at the same locations for case D are compared with those obtained for case B. If the presence of the vertical component of the input motion is considered the permanent horizontal displacement increase by 50% (point K) and 27% (point Q). Finally, Figure 7c shows the vertical displacement computed at the crest of the dam for all the analyses. Negative values indicate settlements. The maximum settlements were obtained for case C (0.57 m) and case A (0.40 m) while about a 50% reduction was observed for case D (0.25 m) and B (0.20 m). As obtained for the acceleration profiles, the minimum values of the settlement were computed for the drained analysis. Even for a return period $T_R = 2475$ years, the maximum settlements were always smaller than the available freeboard (2.6 m).

The displacements showed in Figure 7 result in a overall deformation pattern of the dam which mainly consists of settlements and lateral deformations, with similar values of the horizontal displacement upstream and downstream, as shown Figure 8, which depicts the contour of the horizontal displacement computed for case D.

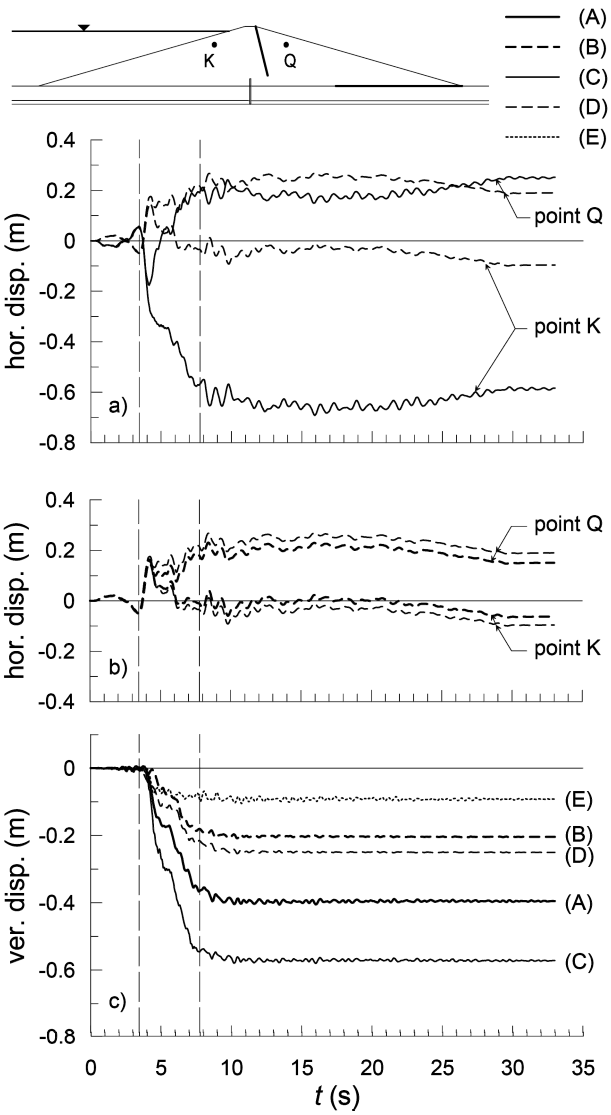

Fig. 7. Horizontal and vertical displacements computed in the 2D dynamic analyses.

IV. CONCLUSIONS

Potential instability of large earth dams existing in Italy represents one of the major source of seismic vulnerability of the Country in that only a few of them were designed accounting for seismic loads explicitly. Hence, it is necessary to investigate the response of most existing earth dams to severe earthquake loading, especially with respect to the deformation patterns that can impair the water retention capabilities of the embankment.

Monitoring data from an existing homogeneous earth dam were used to calibrate a two-dimensional numerical model. Specifically, the settlement of the dam measured during the construction were compared with the computed ones. The seismic behaviour of the dam was

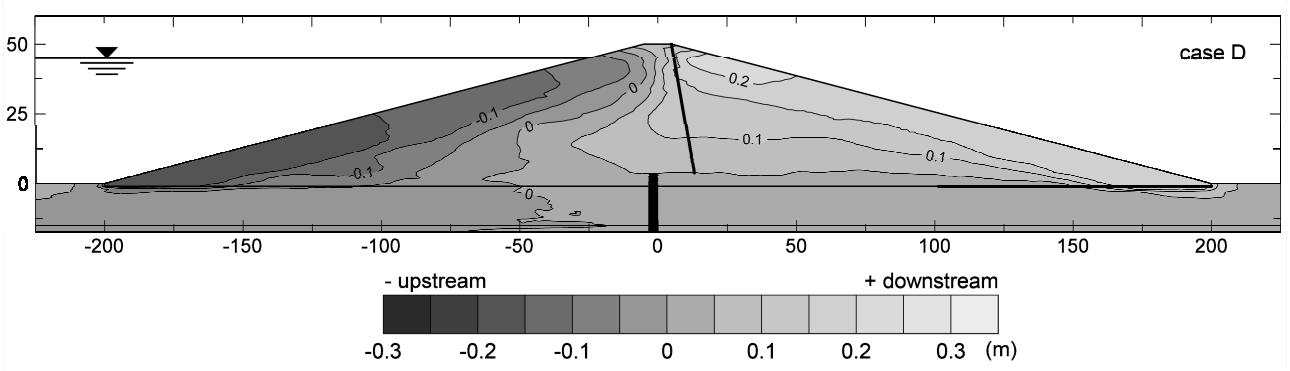

Fig. 8. Dynamic analysis, contours of the horizontal displacements computed for case D at the end of ground motion.

evaluated through a series of dynamic analyses by applying an input motion compatible with the design spectrum specified by the construction code (D.M. 26/06/2014 [10]) for a return period of 2475 years. The results evidenced that taking into account the vertical component of the seismic action induces an increase of the seismic displacements, as higher values of the maximum acceleration develops in the dam body. This effect is sensibly decreased by the assumption of an elastic bedrock. Large amplification effects occur at the crest of the dam for both the acceleration components.

During the seismic shaking, plastic mechanisms are only activated temporarily and the maximum final settlement is smaller than the available freeboard, this confirming the satisfactory performance of the dam in presence of a very severe seismic action.

V. ACKNOWLEDGEMENTS

This research work was partly funded by the Italian Department of Civil Protection under the ReLUIS 2014-2015 research project.

REFERENCES

[1] Itasca (2005). "FLAC Fast Lagrangian Analysis of Continua v. 5.0". User's Manual. Minneapolis, MN, USA: Itasca Consulting Group.

[2] Calabresi G., Rampello S., Sciotti A., Amorosi A. (2000). "Diga sulla Marana Capacciotti: verifica delle condizioni di stabilità e analisi del comportamento in condizioni sismiche". Rapporto di Ricerca Università degli Studi di Roma La Sapienza, Dip. di Ingegneria Strutturale e Geotecnica. A cura e per conto del Consorzio per la Bonifica della Capitanata. Bastogi Editrice, Foggia.

[3] Cascone E., Rampello S. (2003). "Decoupled seismic analysis of an earth dam". Soil Dynamics and Earthquake Engineering, 23 (5): 349-365.

[4] Amorosi, A., Elia, G. (2008). "Analisi dinamica accoppiata della diga Marana Capacciotti". Rivista Italiana di Geotecnica, Patron editore, Bologna, 52 (4): 78-95.

[5] Rampello S., Cascone E., Grosso N. (2009). "Evaluation of the seismic response of a homogeneous earth dam". Soil Dynamics and Earthquake Engineering, 29 (5): 782-798.

[6] Elia G., Amorosi A., Chan A.H.C., Kavvadas M.J. (2010). "Fully coupled dynamic analysis of an earth dam". Géotechnique, 61(7): 549-563.

[7] Callisto L. (2015). "MARTA v. 1.1: a computer program for the site response analysis of a layered soil deposit". https://sites.google.com/a/uniroma1.it/luigicallisto/attivita-1.

[8] Ishibashi, I., Zhang, X. (1993). "Unified dynamic shear moduli and damping ratios of sand and clay". Soils and Foundations, 33(1): 182-191.

[9] Seed H. B., Idriss, I. M. (1979). "Soil moduli and damping factors for dynamic analysis". Report No. EERC 70-10, Berkeley, CA, USA: University of California.

[10] Ministero delle Infrastrutture e dei Trasporti. "D.M. 26/06/2014, Norme tecniche per la progettazione e la costruzione degli sbarramenti di ritenuta (dighe e traverse)" Gazzetta ufficiale della Repubblica Italiana, 156.

[11] Rathje E. M., Abrahamson N. A., Bray, J. D. (1998). "Simplified frequency content estimates of earthquake ground motions". J. Geotech. Geoenviron. Engng, ASCE 124(2): 150–159.

[12] Masini L, Callisto L, Rampello S. (2015). An interpretation of the seismic design of reinforced-earth retaining structures. Geotechnical Earthquake Engineering, Géotechnique symposium in print, 2015. Géotechnique; 65(5):349–358; doi:http://dx.doi.org/ 10.1680/geot./SIP 15-P-001.